



---

*Research article*

## Adaptive neural network control for marine surface vehicles platoon with input saturation and output constraints

Xiaoling Liang<sup>1</sup>, Chen Xu<sup>1</sup> and Duansong Wang<sup>2,\*</sup>

<sup>1</sup> Department of Marine Engineering, Dalian Maritime University, 116026, China

<sup>2</sup> College of Automation, Harbin Engineering University, 150001, China

\* **Correspondence:** Email: wangduansong@hrbeu.edu.cn.

**Abstract:** This paper addresses the decentralized problem for marine surface vessels (MSVs) in the presence of unknown unmodeled nonlinear dynamics, time-varying external disturbances and input saturations. First, platoon formation is proceeded by using line-of-sight (LOS) guidance. Since each marine vehicle can only acquire information from its immediate predecessor, a symmetric barrier Lyapunov function (BLF) is employed to guarantee the formation errors constrained within a certain range such that leaders and followers can preserve the predefined information structure and ensure the correct steady-state regime. Next, due to the superior approximation capability of an adaptive neural network (NN), we propose a BLF-based controller to deal with the model uncertainties. Further, an auxiliary design system is introduced to compensate for the effect of input saturation. Finally, the uniform ultimate boundedness of all the state errors can be proved and simulation examples are presented to illustrate the effectiveness of the proposed method.

**Keywords:** platoon control; marine surface vessels; adaptive neural network control; barrier Lyapunov function; input saturation

**Mathematics Subject Classification:** 93B52, 93C95, 93D05

---

### 1. Introduction

Formation control of multiple marine surface vessels (MSVs) is an important mission in military applications, oceanographic surveys or rescue missions. It has recently attracted considerable attention among researchers [1–3]. Formation problem is a task not only practically interesting but also theoretically significant. From an economic and strategic perspective, marine vessels have to pass some narrow shipping lanes in the world such as the Strait of Malacca, Panama Canal and so on. Thus, platoon formation strategy for marine vessels has obvious benefits in higher efficiency and reduced communication requirements. How to maintain a group of MSVs moving in a platoon

architecture is a motivating example in formation control. Actually, the platoon formation is treated as a decentralized control strategy. Due to the predefined geometry, each vessel can only receive information from its header [4]. Although 1-D longitudinal controllers for linear vehicle models are described in many research literature inherent nonlinearities and uncertainties are essential for most marine vehicle dynamics in practical applications [5, 6].

Unmodeled nonlinear dynamics often exist in marine vehicle systems due to modeling errors, parameter variations or environment disturbances such as wind, wave and ocean currents. Unmodeled nonlinear dynamics are challenging issues because they may severely degrade the performance or even lead to instability of the whole marine vehicle platoon. Therefore, researchers have tried to mitigate the effects of unmodeled nonlinear dynamics. As neural networks have the capability to approximate nonlinear functions, adaptive backstepping approximation-based control design has been widely used for uncertain nonlinear systems [8]. Adaptive neural networks have been adopted to approximate the unknown model parameters of a vessel in [9]. Such adaptive technique is proposed in containment control to compensate for parametric uncertainties [7]. Relative formation applications for this approach and their variants have been developed in [10–12]. Authors have developed the leader-follower formation controller with neural network and dynamic surface control technique to deal with uncertain dynamics in [10]. In [11], using neural networks to estimate the unknown terms, the control schemes achieved distributed tracking for Euler-Lagrange systems. However, compared with the existing literature on the formation with uncertainties, there are relatively few references contributing to marine vessel platoon formation [12].

Another issue associated with a platoon for marine vessels is constraint-based design, such as output constraints, input saturation and so on. Any violation of these constraints would cause the task to fail and threaten marine security. To avoid collisions, a relatively safe space should be considered among MSVs. Meanwhile, to keep effective communication, connectivity between two consecutive vehicles should be maintained during the operation. Therefore, from the practically engineering point of view, output constraints play an important role in formation stability. Artificial potential field [13], prescribed performance [14, 15] and reference governors [16] are some of the existing schemes to handle output constraints. A remarkable technique provided by Prof. Ge using the Barrier Lyapunov Function (BLF) can effectively prevent any violation of output constraints in [18, 19] and marine vessels can be kept moving in a reasonable distance based on BLF. Compared to other schemes, BLF needs less restrictive on initial conditions and does not require the explicit system solution. It is therefore necessary to transfer the constraints of line-of-sight (LOS) range and bearing angle into output constraints. To deal with the connectivity preservation and collision avoidance problems, a linearly transformed error surface was introduced in [20], and to prevent the violations of output constraints, a symmetric barrier Lyapunov function was developed in [21] and trajectory tracking was realized with output constraints. In this paper, the errors combined with BLF are directly used to design the information controller to restrict the distance between two consecutive vehicles within the given zone.

It is noted that input saturation is unavoidable in real applications because of the limited capability of physical actuators. When MSVs maneuver at high speed or suffer from bad sea conditions, drastic changes of control authority often cause saturations which may significantly affect the behaviors of platoons [22, 23]. To deal with this problem, it is necessary to consider input constraints in control design. Many effective methods have been developed to deal with input saturation, such as adaptive compensation [24, 25], model predictive control [26, 27], etc. In some applications, especially

combined with online approximation-based control, tracking the desired performance tends to be controversial. The MPC approach suffers from a heavy computational load. The smooth hyperbolic function and the Nussbaum function are also exploited in [28] to handle the input saturation. However, the derivative of the approximate function leads to challenges in control design and stability analysis. Dealing with the control problem for platoon in the presence of actuator saturation still remains an open problem. In [29], both input saturation and output constraint are dealt with uncertain nonstrict-feedback systems. A fuzzy logic system is employed into the adaptive backstepping technique. In [30], adaptive fuzzy control method is proposed for a class of single-input-single-output (SISO) uncertain nonlinear systems subject to output constraint and input saturation. The unmeasured states are estimated by a fuzzy state observer. In [31], spacecraft rendezvous and proximity operations have been developed with input saturation and full-state constraint. However, relative attitude and position controllers are designed independently and not implemented as an integrated system. Furthermore, although there exist results on input saturation and output constraints, these developed control schemes are seldom applied to the platoon formation problem, especially multiple-input-multiple-output (MIMO) marine vessels.

Motivated by the above considerations, the problem of distributed control design for marine vehicle platoon with unknown external disturbances, output constraints and input saturation is investigated. The intent of this research is motivated by the platooning problem to develop a constraints scheme that provides benefits for MSVs with performance requirements and to design efficient methods such that the cooperating MSVs can maintain the desired platoon architecture and achieve the required performance of the multi-agent systems. The rigorous theoretically handling of input and output constraints in platoon formation control for marine vessels is the main difficulty of the techniques. Constraints on collision avoidance and connectivity maintenance are designed on the performance specification of LOS range and angle. The main contributions of the proposed schemes are highlighted as follows.

[i] The line-of-sight (LOS) range and angle between the multiple marine vessels are constrained to satisfy the formation system specifications or safety requirements. By employing the BLF technique in our platoon control algorithms, the output behavior of MSVs effectively meets the collision and connectivity constraints.

[ii] Adaptive neural network is employed as an effective method for the platoon formation control scheme, which compensates for unmodeled nonlinear dynamics and unknown uncertainties of MSVs, while most of existing works require the ‘linearity-in-parameters’ assumption on MSV systems to handle with the parametric uncertainties.

[iii] The platooning with the effects of saturating nonlinearities has received attention in this paper. Compared with cooperative path following of marine surface in [32], singularity can be avoided in dealing with input saturation. The proposed control schemes can guarantee the string stability of the overall platoon and the uniform ultimate boundedness of all signals.

## 2. Preliminaries and problem description

### 2.1. Preliminaries

**Lemma 1.** [21] For any constant  $x \in \mathbb{R}^n$ , if  $|x| < k$ ,  $k$  is a constant, then the following inequality holds

$$\ln \frac{k^2}{k^2 - x^2} \leq \frac{x^2}{k^2 - x^2}. \quad (2.1)$$

**Lemma 2.** [33] The structure of the neural network is shown in Figure 1. The approximate ability of neural networks had been proved by many researchers. In this work, a class of neural networks with radius basis functions (RBF) is introduced with  $x \in \mathbb{R}^n$ ,  $x$  is the input vector,  $H(x) = [h_1(x), \dots, h_m(x)]^T$  is the output of hidden layer and  $h_j = \exp(-\frac{\|x-c_j\|^2}{2b_j^2})$ ,  $j = 1, 2, \dots, m$ ,  $c_j$  is the center and  $b_j$  is the width of the neural cell in the hidden layer. If  $j$  is chosen large enough, radius basis functions neural network (RBFNN) can approximate any continuous function to an arbitrary accuracy. RBF optimal weight vector is  $W^* = [w_1^*, \dots, w_m^*]^T$ . The weight vector of  $W^*$  is calculated by

$$W^* = \arg \min_{W \in \mathbb{R}^l} \{ \sup_{x \in \Omega} |f(x) - W^T H(x)| \},$$

where node number in the neural network  $l > 1$  and  $W^T H(x)$  can approximate any continuous function  $f(x)$  to any desired accuracy over a compact set  $\Omega \subset \mathbb{R}^n$ . Then the output of RBFNN is

$$f(x) = W^{*T} H(x) + \varepsilon(x),$$

where  $\varepsilon(x)$  denotes the approximate error satisfying  $\varepsilon(x) \leq \bar{\varepsilon}$ , and  $\bar{\varepsilon}$  is an arbitrary small positive constant.

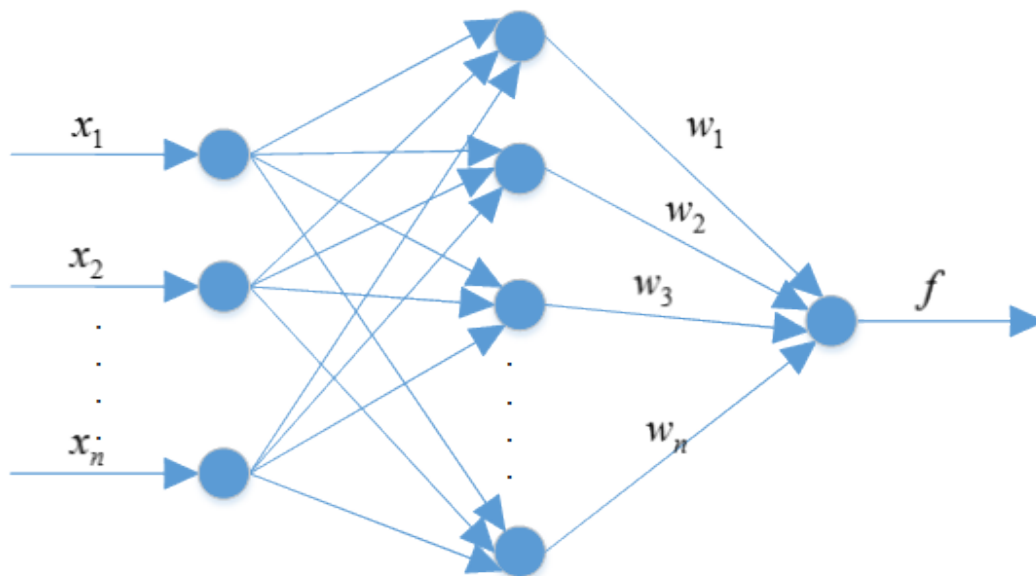


**Figure 1.** The structure of neural network.

## 2.2. Problem description

We consider  $n + 1$  marine surface vehicles labeled as 0 to  $n$ . The formation pattern of this class multiagent system is shown in Figure 2. The kinematics and dynamics of the  $i$ -th MSV can be modeled as follows

$$\dot{\eta}_i = J_i(\eta_i)v_i, \quad (2.2)$$

$$M_i\dot{v}_i = -C_i(v_i)v_i - D_i(v_i)v_i + w_i + \Delta_i + \tau_i, \quad (2.3)$$

where  $\eta_i = [x_i, y_i, \psi_i]^T$  denotes the MSV position and yaw angle with respect to an earth-fixed frame, and  $v_i = [u_i, v_i, r_i]^T$  represents the orientation known as surge, sway and yaw velocities in the body-fixed frame,  $w_i$  is external disturbances induced by wind, wave, and ocean currents, etc,  $\Delta_i$  represents the unmodeled dynamics,  $\tau_{ci}$  denotes the actual control inputs of the  $i$ -th MSV,  $J_i(\psi_i)$  is a nonsingular transformation matrix defined as

$$J_i(\psi_i) = \begin{bmatrix} \cos(\psi_i) & -\sin(\psi_i) & 0 \\ \sin(\psi_i) & \cos(\psi_i) & 0 \\ 0 & 0 & 1 \end{bmatrix} \quad (2.4)$$

$M_i \in \mathbb{R}^{3 \times 3}$  is a symmetric positive definite inertia matrix specified as

$$M_i = \begin{bmatrix} m_{11i} & 0 & 0 \\ 0 & m_{22i} & m_{23i} \\ 0 & m_{32i} & m_{33i} \end{bmatrix} \quad (2.5)$$

where  $m_{11i} = m_i - X_{\dot{u}\dot{u}}$ ,  $m_{22i} = m_i - Y_{\dot{v}\dot{v}}$ ,  $m_{23i} = m_{32i} = m_i x_{gi} - Y_{r\dot{v}}$ ,  $m_{33i} = I_{zi} - N_{r\dot{r}}$ , the mass of the  $i$ -th marine vehicle is  $m_i$  and the  $i$ -th marine vehicle's inertia matrix in the body-fixed frame is  $I_{zi}$ .  $D_i(v_i)$  is hydrodynamic damping matrix specified as

$$D_i(v_i) = \begin{bmatrix} d_{11i} & 0 & 0 \\ 0 & d_{22i} & d_{23i} \\ 0 & d_{32i} & d_{33i} \end{bmatrix} \quad (2.6)$$

where

$$d_{11i}(v_i) = -(X_{u_i} + X_{|u_i|u_i}|u_i| + X_{u_i u_i u_i} u_i^2) \quad (2.7)$$

$$d_{22i}(v_i, r_i) = -(Y_{v_i} + Y_{|v_i|v_i}|v_i| + Y_{|r_i|v_i}|r_i|) \quad (2.8)$$

$$d_{23i}(v_i, r_i) = -(Y_{r_i} + Y_{|v_i|r_i}|v_i| + Y_{|r_i|r_i}|r_i|) \quad (2.9)$$

$$d_{32i}(v_i, r_i) = -(N_{v_i} + N_{|v_i|v_i}|v_i| + N_{|r_i|v_i}|r_i|) \quad (2.10)$$

$$d_{33i}(v_i, r_i) = -(N_{r_i} + N_{|v_i|r_i}|v_i| + N_{|r_i|r_i}|r_i|) \quad (2.11)$$

$C_i(v_i)$  is the matrix of Coriolis and centripetal terms specified as

$$C_i(v_i) = \begin{bmatrix} 0 & 0 & -m_{22i}v_i - m_{23i}r_i \\ 0 & 0 & m_{11i}u_i \\ m_{22i}v_i + m_{23i}r_i & -m_{11i}u_i & 0 \end{bmatrix} \quad (2.12)$$

where the parameters have been shown above. From a practical point of view, the control forces and moments of the marine vessels are limited by the physical properties of thrusters. The saturation nonlinearities can be described as

$$\tau_i = \begin{cases} \tau_{imax}, & \text{if } \tau_{ci} > \tau_{imax} \\ \tau_{ci}, & \text{if } \tau_{imin} < \tau_{ci} < \tau_{imax} \\ \tau_{imin}, & \text{if } \tau_{ci} < \tau_{imin} \end{cases} \quad (2.13)$$

where  $\tau_{imin}$  and  $\tau_{imax}$  respectively stand for the minimum and maximum control forces or moments of vessels' propulsion systems.  $\tau_{ci}$  is the commanded control signals to be designed later.

**Assumption 2.1.** The desired reference trajectory  $\eta_0 = [x_0, y_0, \psi_0]^T$  and its first time derivative  $\dot{\eta}_0$  are bounded functions.

**Assumption 2.2.** There exist known bounded constants  $\tau_{wi}$  for the disturbance term  $w_i$  of each vessel such that

$$w_i \leq \tau_{wi}, i = 0, 1, \dots, n \quad (2.14)$$

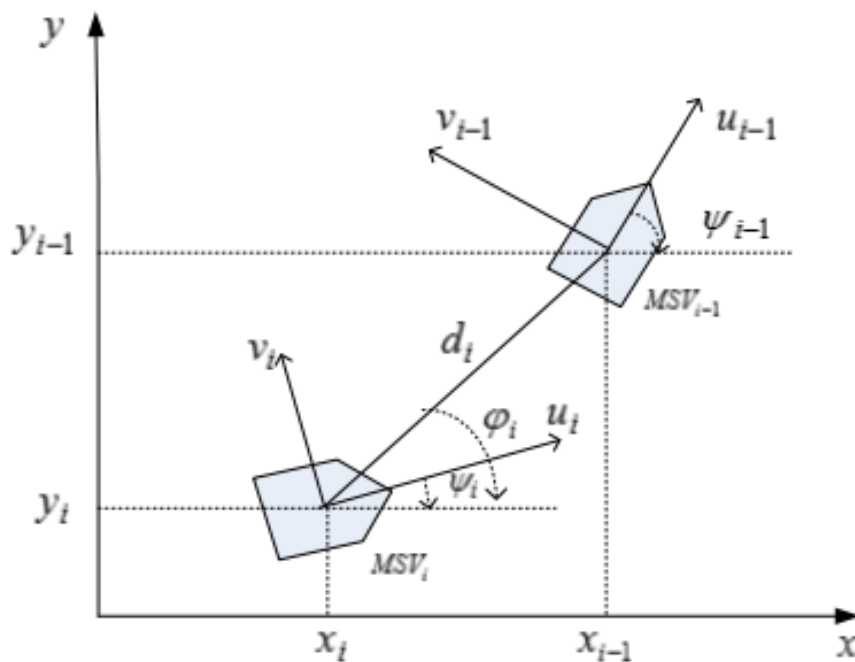


**Figure 2.** MSVs formation configuration.

### 2.3. Formation control with output constraints

In this section, we consider the communications among  $n+1$  MSVs. In each pair of marine vehicles, the follower tries to maintain its LOS range and angle to a desired range and angle relative to its paired-leader. LOS range,  $d_i$ , and angle,  $\varphi_i$ , between two MSVs are defined as

$$d_i = \sqrt{(x_{i-1} - x_i)^2 + (y_{i-1} - y_i)^2}, \quad (2.15)$$

$$\varphi_i = \arctan 2(y_{i-1} - y_i, x_{i-1} - x_i). \quad (2.16)$$

The formation errors of MSVs are designed [21]:

$$\begin{aligned} e_{di} &= d_i - d_{i,des}, \\ e_{\psi_i} &= \psi_{i-1} - \psi_i, \end{aligned} \quad (2.17)$$

where  $d_{i,des}$  is a desired distance between two MSVs. In order to avoid collision avoidance and connectivity maintenance among vehicles, the desired distance during the whole moving process must satisfy the following equations:

$$0 < d_{i,\min col} < d_i \leq d_{i,\max com}, \quad (2.18)$$

where  $d_{i,\min col}$  represents the minimum safety distance and  $d_{i,\max com}$  represents the maximum effective communication distance. For convenience, we define  $\underline{e}_{di}(t) = d_{i,col\min} - d_{i,des}$  as the minimum error distance and  $\bar{e}_{di}(t) = d_{i,col\max} - d_{i,des}$  as the maximum error distance. The bounds of yaw angle errors are defined as  $\bar{e}_{\psi_i}$  and  $\underline{e}_{\psi_i}$ . The constraints of the errors are given as follows:

$$\begin{aligned} -\underline{e}_{di} &< e_{di} < \bar{e}_{di}, \\ -\underline{e}_{\psi_i} &< e_{\psi_i} < \bar{e}_{\psi_i}. \end{aligned} \quad (2.19)$$

To guarantee the output constraints, it is necessary to ensure that the errors defined in (2.17) are not violated and all signals are bounded.

The objective of this paper is to design a control strategy for each vessel described by systems (2.2) and (2.3) to achieve the satisfied distance and angle among MSVs. The followers track the leader's trajectory in platoon formation subject to collision and connectivity constraints. All signals of the closed-loop system in the presence of input saturation are bounded.

### 3. Control design with barrier Lyapunov function

We shall present here an analysis based on the obtained platoon controller structure, and derive an additional set of constraints aimed at satisfying platoon objectives. Let  $z_{1i} = [z_{11i}, z_{12i}]^T = [e_{di}, e_{\psi_i}]^T$ , and  $z_{2i} = v_i - \alpha_i = [z_{21i}, z_{22i}, z_{23i}]^T$ , where  $\alpha_i = [\alpha_{1i}, \alpha_{2i}, \alpha_{3i}]^T$  is a stabilizing function to be designed later. The LOS range should be maintained within the predefined regions between each marine vehicle while the connected platoons track the trajectory. To handle collision avoidance and connectivity between two consecutive agents, BLF is employed to prevent constraint violation in this paper. Consider the symmetric barrier Lyapunov function candidate as

$$V_{1i} = \frac{1}{2} \ln \frac{k_{ai}^2}{k_{ai}^2 - e_{di}^2} + \frac{1}{2} \ln \frac{k_{bi}^2}{k_{bi}^2 - e_{\psi_i}^2}, \quad (3.1)$$

where  $k_{ai}$  and  $k_{bi}$  are positive constants used to constraint  $e_{di}$  and  $e_{\psi_i}$ , i.e.,  $|e_{di}| < k_{ai}$ ,  $|e_{\psi_i}| < k_{bi}$ , respectively. Differentiating of  $V_{1i}$  with respect to time we have

$$\dot{V}_{1i} = \frac{e_{di}\dot{e}_{di}}{k_{ai}^2 - e_{di}^2} + \frac{e_{\psi_i}\dot{e}_{\psi_i}}{k_{bi}^2 - e_{\psi_i}^2}. \quad (3.2)$$

According to (2.17), differentiating  $e_{di}$  and  $e_{\psi_i}$  with respect to time, we can obtain

$$\dot{e}_{di} = -(z_{21i} + \alpha_{1i}) \cos(\psi_i - \varphi_i) + \dot{y}_{i-1} \sin \varphi_i + (z_{22i} + \alpha_{2i}) \sin(\psi_i - \varphi_i) + \dot{x}_{i-1} \cos \varphi_i,$$

$$\dot{e}_{\psi_i} = \dot{\psi}_{i-1} - (z_{23i} + \alpha_{3i}). \quad (3.3)$$

The virtual control  $\alpha_i$  is designed as follows:

$$\begin{aligned} \alpha_{1i} &= \cos(\psi_i - \varphi_i)[k_{di}e_{di}(k_{ai}^2 - e_{di}^2) + \dot{x}_{i-1} \cos \varphi_i + \dot{y}_{i-1} \sin \varphi_i], \\ \alpha_{2i} &= -\sin(\psi_i - \varphi_i)[k_{di}e_{di}(k_{ai}^2 - e_{di}^2) + \dot{x}_{i-1} \cos \varphi_i + \dot{y}_{i-1} \sin \varphi_i], \\ \alpha_{3i} &= k_{\psi_i}e_{\psi_i}(k_{bi}^2 - e_{\psi_i}^2) + \dot{\psi}_{i-1}. \end{aligned} \quad (3.4)$$

Substituting (3.3) and (3.4) into (3.2) yields

$$\dot{V}_{1i} = -k_{di}e_{di}^2 - k_{\psi_i}e_{\psi_i}^2 + \Theta_{1i}, \quad (3.5)$$

where

$$\Theta_{1i} = \frac{e_{di}(-z_{21i} \cos(\psi_i - \varphi_i) + z_{22i} \sin(\psi_i - \varphi_i))}{k_{ai}^2 - e_{di}^2} + \frac{e_{\psi_i}(-z_{23i})}{k_{bi}^2 - e_{\psi_i}^2}. \quad (3.6)$$

The continuous nonlinear function related to the speed  $D_i(v_i)v_i$  and the unmodeled dynamics of the MSV are all unknown. To solve these problems, RBFNN is used to estimate the unknown dynamics and hydrodynamic damping terms. Let

$$W_i^{*T} H_i(Z_i) + \varepsilon_i(Z_i) = -D_i(v_i)v_i + \Delta_i. \quad (3.7)$$

$Z_i = v_i$  is the inputs of the neural network (NN),  $W_i^*$  is the true constant weight value,  $H_i(Z_i)$  is the radial basis function,  $\varepsilon_i(Z_i) \leq \bar{\varepsilon}_i$  is the approximate error,  $\bar{\varepsilon}_i > 0$  is an unknown arbitrary small constant.  $\hat{W}_i^T H_i(Z_i)$  is used to approximate  $W_i^{*T} H_i(Z_i)$ . The adaptive update law is designed as follows:

$$\dot{\hat{W}}_i = \Gamma_i(H_i(Z_i)z_{2i} - \sigma_i|z_{2i}|\hat{W}_i), \quad i = 1, 2, 3, \quad (3.8)$$

where  $\Gamma_i = \Gamma_i^T > 0$  is an adaptive gain matrix and  $\sigma_i$  is a positive constant.

Consider the Lyapunov function candidate  $V_{2i}$

$$V_{2i} = V_{1i} + \frac{1}{2}z_{2i}^T M_i z_{2i} + \frac{1}{2} \sum_{i=1}^3 \tilde{W}_i^T \Gamma_i^{-1} \tilde{W}_i, \quad (3.9)$$

where  $\tilde{W}_i = \hat{W}_i - W_i^*$ . Then the derivation of  $V_{2i}$  is

$$\begin{aligned} \dot{V}_{2i} &= -k_{di}e_{di}^2 - k_{\psi_i}e_{\psi_i}^2 + z_{2i}^T \Theta_{2i} + z_{2i}^T [\tau_i - C_i(v_i)v_i \\ &\quad - M_i \dot{\alpha}_i + \tau_{wi} + W_i^{*T} H_i(Z_i) + \varepsilon_i(Z_i)] + \sum_{i=1}^3 \tilde{W}_i^T \Gamma_i^{-1} \dot{\hat{W}}_i. \end{aligned} \quad (3.10)$$

where

$$\Theta_{2i} = \begin{bmatrix} \frac{-e_{di} \cos(\psi_i - \varphi_i)}{k_{ai}^2 - e_{di}^2} & \frac{e_{di} \sin(\psi_i - \varphi_i)}{k_{ai}^2 - e_{di}^2} & \frac{-e_{\psi_i}}{k_{bi}^2 - e_{\psi_i}^2} \end{bmatrix}^T, \quad (3.11)$$

Due to extreme or varying environments, the external forces such as wind, wave and current are involved in the motion of marine vessels. The saturation of the thrusters needs to be considered and an auxiliary dynamic system is introduced as

$$\dot{\xi}_i = \begin{cases} -K_{\xi_i} \xi_i - \frac{|z_{2i}^T(\eta) \Delta \tau_i| + 0.5 \Delta \tau_i^T \Delta \tau_i}{\|\xi_i\|^2} \xi_i + \Delta \tau_i, & \|\xi_i\| \geq \mu_i \\ 0, & \|\xi_i\| < \mu_i \end{cases} \quad (3.12)$$



where  $\xi_i$  is the state vector of the auxiliary dynamic system,  $\Delta\tau_i = \tau_i - \tau_{ci}$ , and the parameter  $\mu_i$  is a positive constant designed appropriately according to the requirement. The adaptive neural network control law is proposed as follows:

$$\begin{aligned} \tau_{ic} = & (z_{2i}^T)^+ \left( -\frac{k_{di}e_{di}^2}{k_{ai}^2 - e_{di}^2} - \frac{k_{\psi i}e_{\psi i}^2}{k_{bi}^2 - e_{\psi i}^2} \right) + C_i(v_i)v_i - \Theta_{2i} \\ & + M_i\dot{\alpha}_i - \tau_{wi} - K_{2i}(z_{2i} - \xi_i) - \hat{W}_i^T H_i(Z_i), \end{aligned} \quad (3.13)$$

where  $(*)^+$  is the Moore-Penrose pseudoinverse of  $(*)$ ,  $K_{2i} \in \mathbb{R}^{3 \times 3} > 0$ .

Case 1: When  $\|\xi_i\| \geq \mu_i$ , the overall Lyapunov function is

$$V_{3i} = V_{2i} + \frac{1}{2}\xi_i^T \xi_i \quad (3.14)$$

Taking the time derivative of  $V_{3i}$  yields

$$\begin{aligned} \dot{V}_{3i} = & -k_{di}e_{di}^2 - k_{\psi i}e_{\psi i}^2 + z_{2i}^T \Theta_{2i} + z_{2i}^T [\tau_i - C_i(v_i) \\ & - M_i\dot{\alpha}_i + \tau_{wi} + W_i^{*T} H_i(Z_i) + \varepsilon_i(Z_i)] \\ & - \xi_i^T (K_{\xi_i} - \frac{1}{2}I)\xi_i - |z_{2i}^T(\eta)\Delta\tau_i| + \sum_{i=1}^3 \tilde{W}_i^T \Gamma_i^{-1} \dot{\tilde{W}}_i \end{aligned}$$

From Lemma 2, we can know that

$$\begin{aligned} \|\tilde{W}_i\| &= \|\hat{W}_i - W_i^*\| \leq \|\hat{W}_i\| + \|W_i^*\| \\ &\leq \frac{s_i}{\sigma_i} + \|W_i^*\| = \varpi_i. \end{aligned} \quad (3.15)$$

Substituting the control law (3.13), then according to the Young inequality and Lemma 1, we have

$$\begin{aligned} \dot{V}_{3i} \leq & -k_{di} \ln \frac{k_{ai}^2}{k_{ai}^2 - e_{di}^2} - k_{\psi i} \ln \frac{k_{bi}^2}{k_{bi}^2 - e_{\psi i}^2} - \xi_i^T (K_{\xi_i} - \frac{1}{2}I)\xi_i \\ & + z_{2i}^T K_{2i} \xi_i - z_{2i}^T (K_{2i} - I) z_{2i} + \frac{1}{2} \|\varepsilon_i(Z_i)\|^2 \\ & + \sum_{i=1}^3 \frac{\sigma_i^2}{8} (\|W_i^*\|^4 + \frac{\sigma_i^2}{8} \varpi_i^4 - 2\|W_i^*\|^2 \|\tilde{W}_i\|^2) \\ \leq & -k_{di} \ln \frac{k_{ai}^2}{k_{ai}^2 - e_{di}^2} - k_{\psi i} \ln \frac{k_{bi}^2}{k_{bi}^2 - e_{\psi i}^2} + \frac{1}{2} \|\varepsilon_i(Z_i)\|^2 \\ & - \left[ \lambda_{\min}(K_{\xi_i} - \frac{1}{2}K_{2i}) - \frac{1}{2} \right] \xi_i^T \xi_i - \left[ \frac{3}{2} \lambda_{\min}(K_{2i}) - 1 \right] z_{2i}^T z_{2i} \\ & + \sum_{i=1}^3 \frac{\sigma_i^2}{8} (\|W_i^*\|^4 + \frac{\sigma_i^2}{8} \varpi_i^4 - 2\|W_i^*\|^2 \|\tilde{W}_i\|^2). \end{aligned} \quad (3.16)$$

So we can obtain

$$\dot{V}_{3i} \leq -\rho V_{3i} + C, \quad (3.17)$$

where

$$\rho = \min\{2k_{di}, 2k_{\psi i}, \frac{3\lambda_{\min}(K_{2i})-2}{\lambda_{\max}(M_i)}, \frac{\sigma_i^2 \|W_i^*\|^2}{2\lambda_{\max}(\Gamma_i^{-1})}, 2\lambda_{\min}(K_{\xi_i} - \frac{1}{2}K_{2i}) - 1\},$$

$$C = \frac{1}{2}\|\bar{\varepsilon}_i\|^2 + \sum_{i=1}^3 (\frac{\sigma_i^2}{8}\|W_i^*\|^4 + \frac{\sigma_i^2}{8}\varpi_i^4),$$

In this paper, the minimum and maximum eigenvalues of matrix  $\star$  are denoted by  $\lambda_{\min}(\star)$  and  $\lambda_{\max}(\star)$ , respectively.

Case 2: When  $\|\xi_i\| < \mu_i$ ,

$$\xi \dot{\xi} = 0 \quad (3.18)$$

The time derivative of  $V_{3i}$  becomes

$$\begin{aligned} \dot{V}_{3i} &\leq -k_{di} \ln \frac{k_{ai}^2}{k_{ai}^2 - e_{di}^2} - k_{\psi i} \ln \frac{k_{bi}^2}{k_{bi}^2 - e_{\psi i}^2} \\ &\quad - z_{2i}^T (K_{2i} - I) z_{2i} + \frac{1}{2} \|\varepsilon_i(Z_i)\|^2 + z_{2i}^T \Delta \tau_i + z_{2i}^T K_{2i} \xi_i \\ &\quad + \sum_{i=1}^3 \frac{\sigma_i^2}{8} (\|W_i^*\|^4 + \frac{\sigma_i^2}{8} \varpi_i^4 - 2\|W_i^*\|^2 \|\tilde{W}_i\|^2) \\ &\leq -k_{di} \ln \frac{k_{ai}^2}{k_{ai}^2 - e_{di}^2} - k_{\psi i} \ln \frac{k_{bi}^2}{k_{bi}^2 - e_{\psi i}^2} \\ &\quad - z_{2i}^T (K_{2i} - I) z_{2i} + \frac{1}{2} \|\varepsilon_i(Z_i)\|^2 + \frac{3}{2} z_{2i}^T z_{2i} \\ &\quad + \frac{1}{2} \|\Delta \tau_i\|^2 - \frac{1}{2} \xi_i^T K_{2i}^T K_{2i} \xi_i + \mu_i^2 \|K_{2i}^T K_{2i}\| \\ &\quad + \sum_{i=1}^3 \frac{\sigma_i^2}{8} (\|W_i^*\|^4 + \frac{\sigma_i^2}{8} \varpi_i^4 - 2\|W_i^*\|^2 \|\tilde{W}_i\|^2) \\ &\leq -\rho V_{3i} + C \end{aligned} \quad (3.19)$$

where

$$\rho = \min\{2k_{di}, 2k_{\psi i}, \frac{2\lambda_{\min}(K_{2i}-5)}{\lambda_{\max}(M_i)}, \frac{\sigma_i^2 \|W_i^*\|^2}{2\lambda_{\max}(\Gamma_i^{-1})}, \lambda_{\min}(K_{2i}^T K_{2i})\},$$

$$C = \frac{1}{2}\|\bar{\varepsilon}_i\|^2 + \sum_{i=1}^3 (\frac{\sigma_i^2}{8}\|W_i^*\|^4 + \frac{\sigma_i^2}{8}\varpi_i^4) + \frac{1}{2}\|\Delta \tau_i\|^2 + \mu_i^2 \|K_{2i}^T K_{2i}\|.$$

It is obvious that for all  $V(0) < B_0$ ,  $B_0$  being any positive constant, all signals are guaranteed to be uniformly ultimately bounded [34, 35]. Therefore, there is the following theorem

**Theorem 1.** Consider a string of  $n + 1$  MSVs in (2.2)–(2.3) with unmodeling uncertainties, external disturbance and input saturations under Assumption 2.1 and 2.2, the virtual control (3.4), the robust control law (3.13), the adaption law (3.7) and the auxiliary dynamic system (3.12), such that all signals in the closed-loop system under the initial condition  $V(0)$  can be guaranteed to be uniformly ultimately bounded while collision avoidance and connectivity maintenance satisfy the constraints by appropriately adjusting the design parameters.

#### 4. Simulation examples

In this section, a string of 4 MSVs are used in numerical simulations to demonstrate the effectiveness of the proposed method. The communication relationship of 4 MSVs is shown in Figure 3.

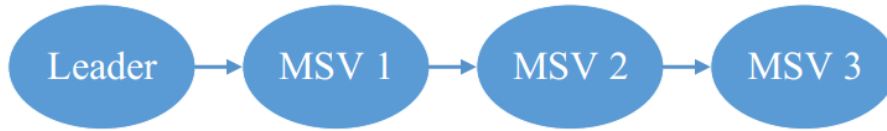


**Figure 3.** Communication graph among the MSVs.

The marine vehicle model used for simulation in this work is Cybership-II, which is a 1:70 scale supply vessel replica built in a marine control laboratory in the Norwegian University of Science and Technology [36]. For the sake of convenience in comparison, the desired reference trajectory is chosen the same as that in [12], where  $t_c \geq 0$  is a time constant and  $t' = 0.02(t - t_c)$ . The desired distance between the follower and the leader is considered as 5m. The initial states of the MSVs are given as  $\eta_0 = [0, 0, 0]^T$ ,  $\eta_1 = [0, 5, 0]^T$ ,  $\eta_2 = [0, 10, 0]^T$ ,  $\eta_3 = [0, 15, 0]^T$  and  $v_1 = v_2 = v_3 = [0, 0, 0]^T$ . The time constant  $t_c = 200$  s. Figure 3 shows the validity of the position and velocity information among the MSVs. The minimum collision distance is set at 4m and the maximum connectivity distance is chosen as 6m. So the distance error should satisfy following constraints:

$$d_{i,col\ min} < d_i < d_{i,con\ max}, i = 1, 2, 3.$$

If the inequality satisfies the constraints during the whole moving process, it means that the collision distance and effective connectivity distance will not be violated, so the output constraints can be guaranteed.

Simulation parameters are chosen as follows:  $k_{d1} = 11, k_{d2} = k_{d3} = 3, k_{\psi1} = 1, k_{\psi2} = k_{\psi3} = 0.5, k_{a1} = k_{a2} = k_{a3} = 1$  and  $k_{b1} = k_{b2} = k_{b3} = 0.5$ . The control gains are set as  $\text{diag}\{6, 6, 4\}$ . The neural network inputs are chosen as  $Z_{i1} = u_i$  and  $Z_{i2} = Z_{i3} = [v_i, r_i]^T, i = 1, 2, 3$ . In the simulation section, we construct RBFNN  $\hat{W}_{1i}^T S_{1i}(Z_{1i})$  using 27 nodes, with centers evenly spaced on  $[0, 2.4]$  and width being 0.1,  $\hat{W}_{2i}^T S_{2i}(Z_{2i})$  using 49 nodes, with centers evenly spaced on  $[-2, 2] * [-2, 2]$  and width being 0.1,  $\hat{W}_{3i}^T S_{3i}(Z_{3i})$  using 49 nodes, with centers evenly spaced on  $[-1.5, 1.5] * [-1.5, 1.5]$  and width being 0.2. From Figure 4, it is obvious that the MSVs can move in a desired formation pattern. Each marine vehicle follows its preceding surface vessel's trajectory under the external disturbance and unknown dynamics. Figure 5 shows that though the hydrodynamic damping matrix  $D_i$  is unknown to input  $\tau_i$ , through NN learning LOS range  $d_i$  converges to a small neighborhood of the desired distance and the error satisfies the predefined boundary restriction, which means that during the whole process the distance between the successive vehicles does not violate the collision and connectivity constraints. We can observe from Figure 6, the distance between the successive vehicles is limited within 4 m (collision avoidance distance) to 6 m (the maximum connection distance) during the whole moving process. So the distance error constraints satisfy the design requirement  $-k_{ai} < e_{di} < k_{ai}, i = 1, 2, 3$ . Figure 7 shows that the control inputs of each marine vehicle achieve satisfied control performances. Adaptive neural network based formation control scheme for autonomous marine surface vehicles is

developed in [12]. The simulation result is shown in Figure 2(a), where the tracking trajectories for five unmanned surface vehicles along with the desired reference trajectory. Compared with the adaptive control technique in [12], the performance of the proposed technique shown in Figure 4 is better than the one in [12]. In addition, the input and output constraints of the platoon formation are guaranteed at the same time in the simulation example. The simulation results illustrate the effectiveness of the proposed adaptive control method in platoon formation.

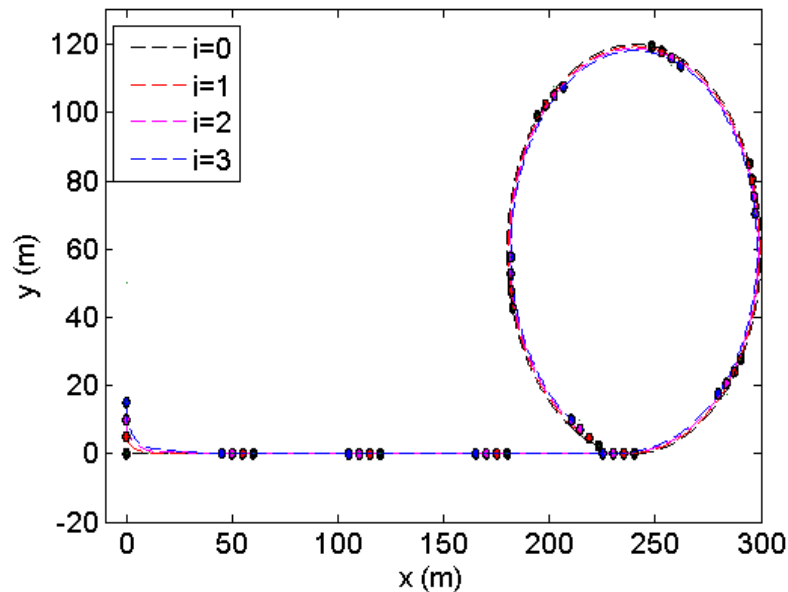


**Figure 4.** The north-east position of the 4 MSVs under NN adaptive control.

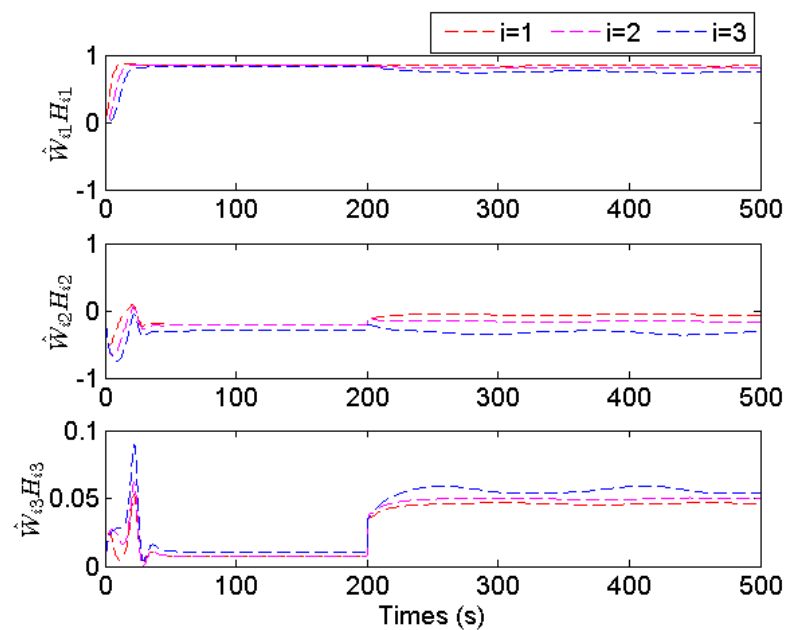


**Figure 5.** NN estimate value.

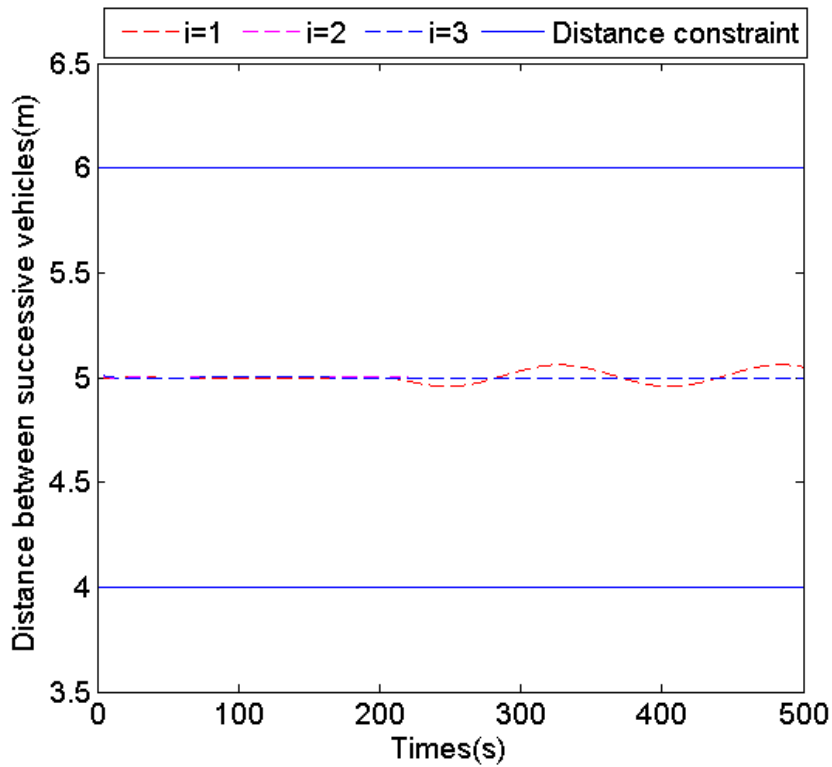


**Figure 6.** LOS range  $d_i$ , the maximum connectivity distance and minimum collision distance.

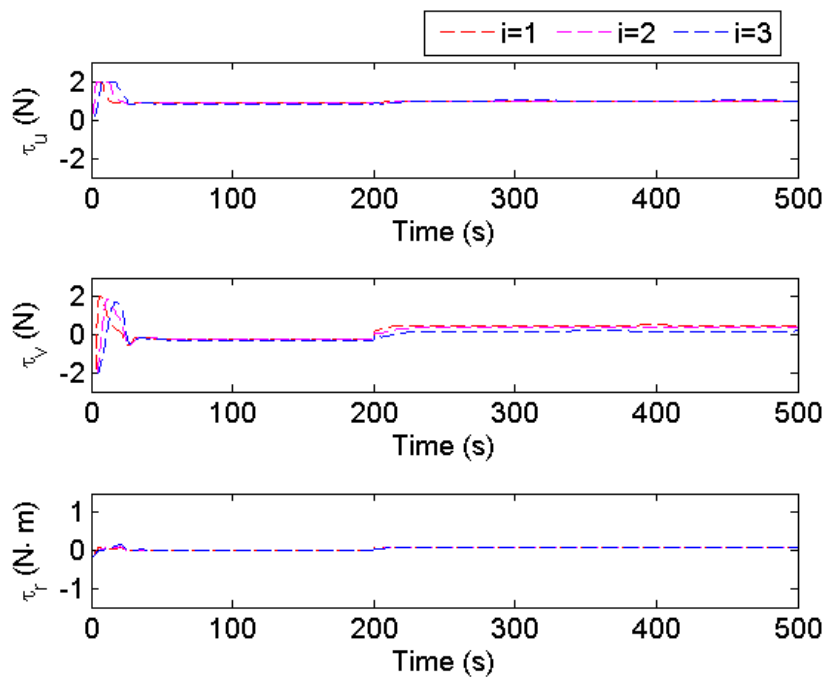


**Figure 7.** Control Input.

## 5. Conclusions

In this paper, a formation control scheme for autonomous marine surface vehicles with model uncertainties and constraints has been addressed by combining the BLF technique and adaptive NN. Collision avoidance and connectivity maintenance have been transferred into the LOS range and angle error constraints. To prevent any violation of constraints, the proposed algorithm based on BLF was designed by backstepping control. The adaptive NN was presented to approximate uncertain model dynamics. Input saturation was considered for marine vessels and a compensated control law was adopted in the control design. The uniform ultimate boundedness of all the state errors have been proven by stability analysis. Simulation studies have been carried out to illustrate the feasibility of the proposed approach. In the future, more practical research will be considered, such as the effect of measurement noise, the communication constraints, and so on.

## Acknowledgments

This research was funded by Liaoning Province Natural Science Foundation Under Grant 20170520430 and the Fundamental Research Funds for the Central Universities Under Grant 3132018253. The authors would like to thank the editors and reviewers for the constructive comments and kind support to improve the quality of this paper.

## Conflict of interest

The authors declare no conflict of interest.

## References

1. Y. Liu, Z. Geng, *Finite-time optimal formation tracking control of vehicles in horizontal plane*, *Nonlinear Dynam.*, **76** (2014), 481–495.
2. T. P. Nascimento, L. F. S. Costa, A. G. S. Conceição, et al. *Nonlinear model predictive formation control: An iterative weighted tuning approach*, *J. Intell. Robot. Syst.*, **80** (2015), 441–454.
3. Q. Wang, Y. Wang, H. Zhang, *The formation control of multi-agent systems on a circle*, *IEEE/CAA J. Autom. Sin.*, **5** (2016), 148–154.
4. B. Das, B. Subudhi, B. B. Pati, *Cooperative formation control of autonomous underwater vehicles: An overview*, *Int. J. Autom. comput.*, **13** (2016), 199–225.
5. S. S. Stankovic, M. J. Stanojevic, D. D. Siljak, *Decentralized overlapping control of a platoon of vehicles*, *IEEE T. Contr. Syst. T.*, **8** (2000), 816–832.
6. H. Li, Y. Shi, W. Yan, *Distributed receding horizon control of constrained nonlinear vehicle formations with guaranteed  $\gamma$ -gain stability*, *Automatica*, **68** (2016), 148–154.
7. S. J. Yoo, B. S. Park, *Guaranteed performance design for distributed bounded containment control of networked uncertain underactuated surface vessels*, *J. Franklin I.*, **354** (2017), 1584–1602.

8. Q. Hou, J. Dong, *Adaptive fuzzy reliable control for switched uncertain nonlinear systems based on closed-loop reference model*, Fuzzy Set. Syst., DOI: <https://doi.org/10.1016/j.fss.2019.04.016>.
9. W. He, Z. Yin, C. Sun, *Adaptive neural network control of a marine vessel with constraints using the asymmetric barrier Lyapunov function*, IEEE T. Cybernetics, **47** (2016), 1641–1651.
10. Z. Peng, D. Wang, Z. Chen, et al. *Adaptive dynamic surface control for formations of autonomous surface vehicles with uncertain dynamics*, IEEE T. Contr. Syst. T., **21** (2012), 513–520.
11. L. Chen, C. Li, Y. Sun, et al. *Distributed finite-time tracking control for multiple uncertain Euler-Lagrange systems with input saturations and error constraints*, IET Contr. Theory Appl., **13** (2018), 123–133.
12. S. Dai, S. He, H. Lin, et al. *Platoon formation control with prescribed performance guarantees for USVs*, IEEE T. Ind. Electron., **65** (2018), 4237–4246.
13. E. Rimon, D. E. Koditschek, *Exact robot navigation using artificial potential functions*, IEET T. Robotic. Autom., **8** (1992): 501–518.
14. C. P. Bechlioulis, G. A. Rovithakis, *Robust adaptive control of feedback linearizable MIMO nonlinear systems with prescribed performance*, IEEE T. Automat. Contr., **53** (2008), 2090–2099.
15. J. Na, Q. Chen, X. Ren, et al. *Adaptive prescribed performance motion control of servo mechanisms with friction compensation*, IEEE T. Ind. Electron., **61** (2013), 486–494.
16. E. G. Gilbert, I. Kolmanovsky, K. T. Tan, *Nonlinear control of discrete-time linear systems with state and control constraints: A reference governor with global convergence properties*, In: *Proceedings of 1994 33rd IEEE Conference on Decision and Control*, IEEE, **1** (1994), 144–149.
17. E. Gilbert, I. Kolmanovsky, *Nonlinear tracking control in the presence of state and control constraints: A generalized reference governor*, Automatica, **38** (2002), 2063–2073.
18. D. Li, G. Ma, C. Li, et al. *Distributed attitude coordinated control of multiple spacecraft with attitude constraints*, IEEE T. Aero. Elec. Syst., **54** (2018): 2233–2245.
19. K. P. Tee, S. S. Ge, E. H. Tay, *Barrier Lyapunov functions for the control of output-constrained nonlinear systems*, Automatica, **45** (2009), 918–927.
20. B. S. Park, S. J. Yoo, *An error transformation approach for connectivity-preserving and collision-avoiding formation tracking of networked uncertain underactuated surface vessels*, IEEE T. Cybernetics, **49** (2018), 2955–2966.
21. Z. Zhao, W. He, S. S. Ge, *Adaptive neural network control of a fully actuated marine surface vessel with multiple output constraints*, IEEE T. Contr. Syst. T., **22** (2014), 1536–1543.
22. B. Zhou, X. Yang, *Global stabilization of the multiple integrators system by delayed and bounded controls*, IEEE T. Automat. Contr., **61** (2015), 4222–4228.
23. X. Liang, M. Hou, G. Duan, *Adaptive dynamic surface control for integrated missile guidance and autopilot in the presence of input saturation*, J. Aerospace Eng., **28** (2014), 04014121.
24. W. He, Y. Dong, C. Sun, *Adaptive neural impedance control of a robotic manipulator with input saturation*, IEEE T. Syst. Man Cy. S., **46** (2015), 334–344.
25. H. Wang, X. Liu, K. Liu, *Adaptive neural data-based compensation control of non-linear systems with dynamic uncertainties and input saturation*, IET Contr. Theory Appl., **9** (2015), 1058–1065.

26. D. Q. Mayne, J. B. Rawlings, C. V. Rao, et al. *Constrained model predictive control: Stability and optimality*, *Automatica*, **36** (2000), 789–814.
27. X. Liang, M. Hou, H. Guo, *A continuous predictive approach based on backstepping with application to integrated guidance and control design*, In: *35th Chinese Control Conference*, IEEE, 2016, 10870–10874.
28. N. Ji, J. Liu, *Vibration control for a flexible satellite with input constraint based on Nussbaum function via backstepping method*, *Aerosp. Sci. Technol.*, **77** (2018), 563–572.
29. Q. Zhou, L. Wang, C. Wu, et al. *Adaptive fuzzy control for nonstrict-feedback systems with input saturation and output constraint*, *IEEE T. Syst. Man Cy. S.*, **47** (2016), 1–12.
30. Y. Li, S. Tong, T. Li, *Adaptive fuzzy output-feedback control for output constrained nonlinear systems in the presence of input saturation*, *Fuzzy Set. Syst.*, **248** (2014), 138–155.
31. L. Sun, W. Huo, Z. Jiao, *Adaptive backstepping control of spacecraft rendezvous and proximity operations with input saturation and full-state constraint*, *IEEE T. Ind. Electron.*, **64** (2016), 480–492.
32. H. Wang, D. Wang, Z. Peng, *Adaptive dynamic surface control for cooperative path following of marine surface vehicles with input saturation*, *Nonlinear Dynam.*, **77** (2014), 107–117.
33. W. He, S. S. Ge, Y. Li, et al. *Neural network control of a rehabilitation robot by state and output feedback*, *J. Intell. Robot. Syst.*, **80** (2015), 15–31.
34. D. Li, W. Zhang, W. He, et al. *Two-layer distributed formation-containment control of multiple Euler-Lagrange systems by output feedback*, *IEEE T. Cybernetics*, **49** (2018), 675–687.
35. W. Ren, Y. Cao, *Distributed Coordination of Multi-Agent Networks: Emergent Problems, Models, and Issues*, Springer Science & Business Media, 2010.
36. K. P. Tee, S. S. Ge, *Control of fully actuated ocean surface vessels using a class of feedforward approximators*, *IEEE T. Contr. Syst. T.*, **14** (2006), 750–756.



AIMS Press

©2020 the Author(s), licensee AIMS Press. This is an open access article distributed under the terms of the Creative Commons Attribution License (<http://creativecommons.org/licenses/by/4.0>)